Talanta 239 (2022) 123083

Contents lists available at ScienceDirect

Talanta

journal homepage: www.elsevier.com/locate/talanta

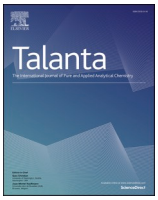

Disposable biosensor based on novel ternary Ru-PEI@PCN-333(Al) self-enhanced electrochemiluminescence system for on-site determination of caspase-3 activity

Weiwei Luo [a,c], Hongyu Chu [b], Xinzhao Wu [a], Pinyi Ma [a,**], Qiong Wu [b,***], Daqian Song [a,*]

[a] College of Chemistry, Jilin Province Research Center for Engineering and Technology of Spectral Analytical Instruments, Jilin University, Qianjin Street 2699, Changchun, 130012, China
[b] Department of Gastrointestinal and Colorectal Surgery, China-Japan Union Hospital of Jilin University, Sendai Street 126, Changchun, 130033, China
[c] School of Chemistry and Life Science, Anshan Normal University, Ping'an Street 43, Anshan, 114005, China

ARTICLE INFO

Keywords:
Caspase-3
Apoptosis
Electrochemiluminescence (ECL)
Metal organic frameworks (MOFs)
Screen-printed electrodes (SPEs)
Electrochemical sensors
Biosensor

ABSTRACT

The number of death due to cancer-related diseases each year is at the alarming level and is constantly growing. Tools that can effectively and conveniently detect cancer cell apoptosis can play a significant role in cancer research, cancer therapy, and other related industries. Herein, we fabricated, for the first time, an ultrasensitive, disposable, self-enhanced off-on electrochemiluminescence (ECL) biosensor based on ternary Ru-PEI@PCN-333 (Al) system to determine caspase-3 activity, the biomarker of apoptosis. The biosensor had a low detection limit of 0.017 pg/mL and was able to enhance the ECL emission and stability. A solid-state (SS) ECL strategy was adopted to overcome the relatively weak ECL emission due to the long distance between electrochemiluminophore and electrode surface. The analysis requires only one incubation step, which can significantly reduce the operational complexity and time. The biosensor had higher sensitivity, and the off-on ECL mode was achieved using caspase-3 as a switch. The on-site and rapid detection capability of the biosensor was achieved by the introduction of disposable screen-printed electrodes (SPEs). This study lays a foundation for the development of more advanced, ingenious, portable and reliable ECL devices for biosensing not only caspase-3, but also other bioanalytes.

1. Introduction

Detection of various cancer biomarkers is indispensable for the success of cancer diagnosis and treatment [1]. In cancer therapies, the ability to monitor cancer cell apoptosis is also important in order to effectively evaluate the elimination of cancer cells [2–4]. Therefore, a biomarker of cancer cell apoptosis, caspase-3 (~17 kDa, a member of the protease caspases family), has received considerable attention from analytical chemists in the past few years [5–7]. Thus, it is imperative to develop analytical methods that can sensitively determine caspase-3 activity [8]. Caspase-3 can specifically recognize and cleave the Asp-Glu-Val-Asp (DEVD) tetrapeptide sequence, and hydrolyze the peptide bond behind the C-terminal Asp residue [9,10]. Many analytical methods have been applied in caspase-3 activity determination, such as colorimetric [11], fluorometric [12], chemiluminescence [13], and electrochemical [14] methods. These methods, however, still have some limitations. Whereas colorimetry and chemiluminescence have relatively low sensitivity, fluorometric method is laborious and time-consuming. Although electrochemical methods have high sensitivity, the interference by mixed signals at the electrode interface is often difficult to be suppressed.

Electrochemiluminescence (ECL) refers to the process in which species generated at electrodes undergo high-energy electron-transfer reactions to reach their excited states while emitting light [15]. Because of the separation of excitation energy source (electricity) and detection signal (light), ECL has high sensitivity and near-zero background; therefore, it has been applied in many analytical fields [16,17]. Numerous ECL biosensors for determining caspase-3 activity have been

* Corresponding author.
** Corresponding author.
*** Corresponding author.
E-mail addresses: mapinyi@jlu.edu.cn (P. Ma), qiong_wu@jlu.edu.cn (Q. Wu), songdq@jlu.edu.cn (D. Song).

https://doi.org/10.1016/j.talanta.2021.123083
Received 21 October 2021; Received in revised form 16 November 2021; Accepted 17 November 2021
Available online 19 November 2021

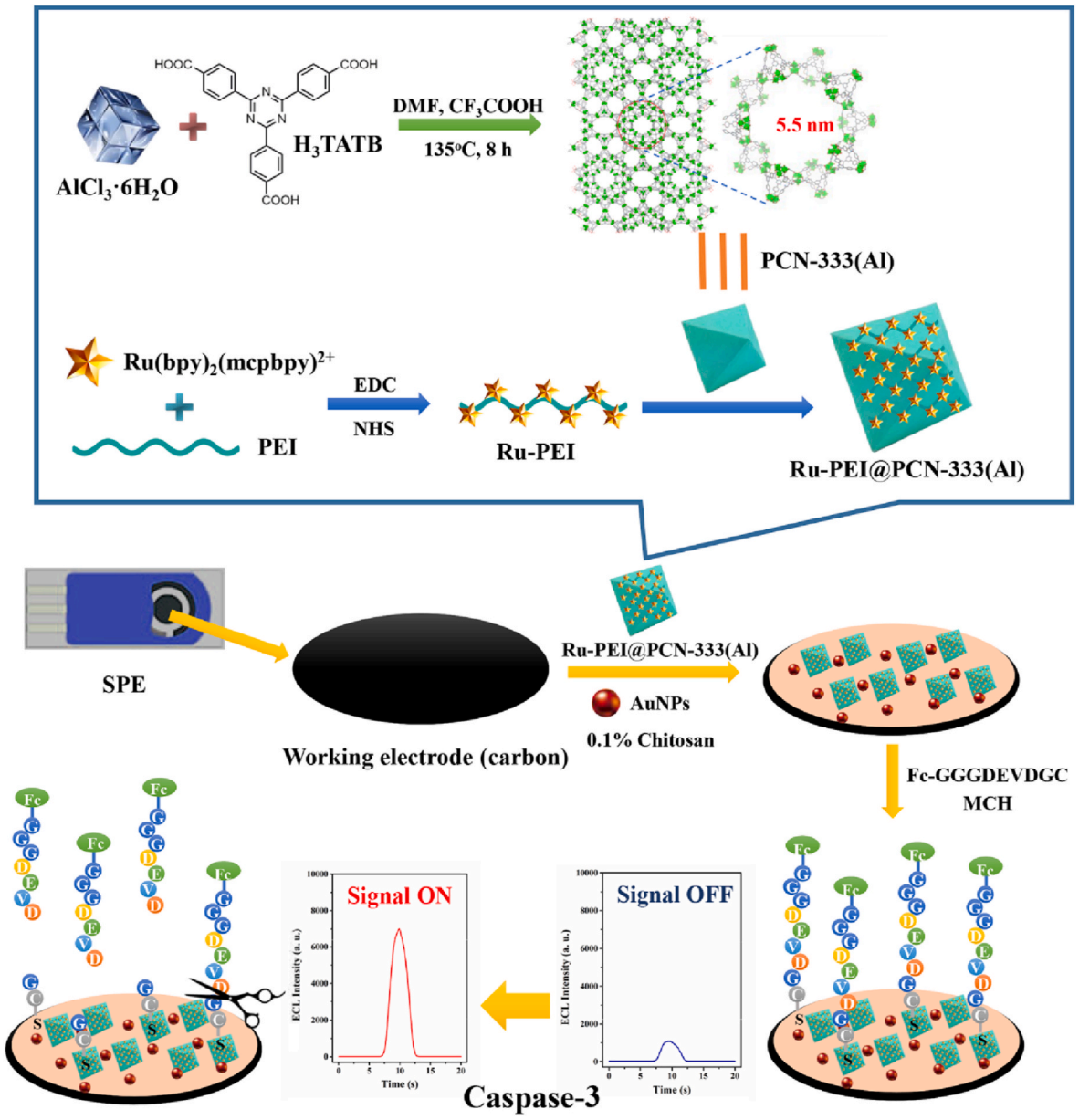

Scheme 1. Preparation of Ru-PEI@PCN-333(Al) and construction of ECL biosensor for caspase-3 detection.

fabricated. Khalilzadeh et al. [18] have fabricated an ECL biosensor for caspase-3 activity determination using luminol-horseradish peroxidase enzyme (HRP)-H_2O_2 ECL system and achieved the limit of detection (LOD) of 0.5 fM. Dong et al. [6] have fabricated an ECL biosensor for detecting caspase-3 activity using Ru@SiO_2-TPA ECL system and achieved the LOD of 0.07 pg/mL. However, the liquid-state ECL used in their designs causes the efficiency of luminophore utilization and the ECL emission due to the long distance between electrode surface and luminophores to decrease. Additionally, the method requires a large amount of enzymes and coreactants during the measurements, which increases the instability and inconvenience of the ECL biosensor. Besides, two or more incubation steps are needed in the measurements, thus the operation time is prolonged. Better strategies and ECL systems for sensing caspase-3 activity should be designed and introduced.

Intramolecular self-enhanced ECL is the strategy in which luminophores and their co-reactive groups are embedded in the same structure to shorten the electronic transmission distance, improve the luminous stability and enhance the luminous efficiency [19]. Many self-enhanced ECL complexes have been developed, such as Ru-PEI [20], ABEI-Cys [21], and AuNCs-DPEA [22]. Among all the complexes, Ru-PEI, which has an abundance of surface binding sites, is more widely used. Moreover, these self-enhanced ECL complexes are often grafted or immobilized onto various nanomaterials to further enhance the ECL performance. For example, Cao et al. [23] have constructed a PEI-CdS/Au@SiO_2@RuDS self-enhanced ECL system via electrostatic interaction between PEI-CdS QDs and Au@SiO_2@$Ru(bpy)_3^{2+}$-doped silica. Ye et al. [24] have constructed a Ru-BCDs self-enhanced ECL system by covalently linking BPEI-coated carbon dots (BCDs) with $Ru(dcbpy)_3^{2+}$. The enhanced ECL properties of both self-enhanced ECL systems are proven to originate from the synergistic effects between the components.

As an emerging porous crystalline material, metal–organic frameworks (MOFs) have received increasing attention and have been applied in many fields such as biosensing [25–27]. However, the application of MOFs in ECL biosensing is usually limited by their poor conductivity [25]. In order to overcome this limitation, ECL-active MOF-based composites with higher loading capacity, conductivity and luminous efficiency have been synthesized and achieved by methods such as

post-synthetic modification [26]. PCN-333(Al) (PCN stands for porous coordination network) with ultra-large mesoporous cages (5.5 nm), high void volumes (3.84 cm^3/g), and good chemical stability in aqueous solutions have been shown to have excellent enzyme loading [28]. For ECL biosensing, PCN-333(Al) with unique caged and reticulated structure may be used as a scaffold for the loading of multiple self-enhanced ECL composites to construct a self-enhanced ECL system or ECL-active MOF based composites. Herein, we designed a Ru-PEI@PCN-333(Al) ternary self-enhanced ECL system by linking ECL luminescent materials Ru $(bpy)_2(mcpbpy)^{2+}$ with polyethyleneimine (PEI) via amide bonds, PEI as coreactant can enhance the ECL efficiency of the luminescent materials. Then, the positively charged Ru-PEI was immobilized onto the negatively charged PCN-333(Al) via electrostatic interaction to form the Ru-PEI@PCN-333(Al) ternary self-enhanced ECL system. PCN-333(Al) can immobilize ECL luminescent materials, and has a certain channel restriction enhancement effect. In addition, CS acts as a binder to fix PCN-333(Al) on the electrode. This ternary self-enhanced ECL system had excellent stability and high ECL emission, thus could greatly improve the sensitivity of the biosensor.

Inspired by the increasing demand for point-of-care testing (POCT) systems [29–32], we introduced screen-printed electrodes (SPEs) into our biosensor in order to rapidly perform on-site caspase-3 activity determination in the monitoring of cell apoptosis. This is the first ultrasensitive disposable biosensor for rapid determination of caspase-3 activity with well-designed interface systems and sensing strategies. The preparation process and detection mechanism of the ECL biosensor are shown in Scheme 1. Firstly, the constructed self-enhanced ternary Ru-PEI@PCN-333(Al) ECL system was modified on the surface of SPEs to form solid-state ECL-modified electrodes; the immobilization stability and glaring ECL emission were excellent. With a designed ferrocene (Fc)-terminated peptide, Fc-GGGDEVDGC, an off-on strategy could be achieved using caspase-3 as an ECL switch to turn on the intensity of ECL. The oxidation product of Fc on the electrode, Fc+, reacts with the excited state [Ru2+-PEI@PCN-333(Al)]* to quench ECL luminescence [33]. With this strategy, the analysis becomes simpler, as it only requires one incubation step, and the operation time can be reduced. The analytical performance of the disposable ECL-based caspase-3 biosensor was examined and found to have the detection limit of 0.017 pg/mL and be able to detect caspase-3 in real MOLM-13 cell samples. We further explored its performance in monitoring the apoptosis of acute myeloid leukemia cells induced by two anti-cancer drugs, daunorubicin and adriamycin. Our biosensor can be developed into more advanced portable ECL biosensing devices for detecting caspase-3 and other bioanalytes.

2. Experimental section

2.1. Synthesis of PCN-333(Al)

PCN-333(Al) was synthesized by a solvothermal method [28] through reactions between H_3TATB and $AlCl_3$. Firstly, 50 mg of H_3TATB and 200 mg of $AlCl_3{\cdot}6H_2O$ were dissolved in 10 mL of DMF, and 1.0 mL of trifluoroacetic acid was then added. The mixture was heated at 135 °C in an oven for 48 h until white precipitate was formed. The precipitate was centrifuged and washed 3 times with freshly prepared DMF, after which white powder of PCN-333(Al) was obtained.

2.2. Synthesis of Ru-PEI@PCN-333(Al)

Firstly, 14.8 mg of $[Ru(bpy)_2(mcpbpy)]Cl_2$ was dissolved in 4 mL of ultrapure water, after which 57.6 mg of EDC and 11.6 mg of NHS were added to activate the carboxyl groups of $[Ru(bpy)_2(mcpbpy)]Cl_2$, and the mixture was stirred for 30 min. Subsequently, PEI solution (1%, MW = 1800) was added, and the mixture was stirred for another 2 h to obtain the Ru-PEI complex. After 10 mg of negatively charged PCN-333(Al) was added, the mixture was further stirred for 24 h. The obtained mixture was dialyzed using a dialysis bag (molecular weight cut-off = 8000–14000) for 24 h and then concentrated by centrifugation. The obtained Ru-PEI@PCN-333(Al) was redispersed in 1 mL of ultrapure water and then stored at 4 °C in darkness until use.

2.3. Synthesis of AuNPs

AuNPs with a diameter of ~12 nm were synthesized according to the method described in the literature [34]. Briefly, 4.0 mL of 1% trisodium citrate was added into 100 mL of boiling 0.01% $HAuCl_4$ aqueous solution under vigorously stirring. The mixture was then stirred and boiled for 30 min, and AuNPs were obtained after the mixture solution was cooled to room temperature. The obtained AuNPs were stored at 4 °C in darkness until further use.

2.4. Fabrication of disposable caspase-3 ECL biosensor

The disposable caspase-3 ECL biosensor was fabricated by the use of SPEs. SPEs were prepared from polyethylene terephthalate, and the system consisted of three integrated electrodes: working electrode (carbon), counter electrode (carbon) and reference electrode (Ag/AgCl). Before the modification, the SPEs were first pretreated with 0.05 M H_2SO_4 solution under cyclic voltammetry (CV) scanning between 0.5 and 1.1 V until the CV curve measured at a scanning speed of 0.1 V/s was stable. The SPEs were then washed successively with ultrapure water, alcohol and a mixture of ultrapure water and alcohol at a volume ratio of 1:1. After these steps, the SPEs were dried and stored until further use [35].

For the modification, 0.5 mL of Ru-PEI@PCN-333(Al), 0.4 mL of AuNPs, and 0.1 mL of 0.1% chitosan (CS) solution were mixed and stirred for 30 min to obtain the modifying liquid. After that, 10 μL of the modifying liquid was carefully coated on the surface of SPE by drop-casting. The SPE was air-dried until a uniform AuNPs/Ru-PEI@PCN-333(Al)/CS film was visibly formed on its surface. After the film was completely dried, 10 μL of Fc-peptide (10 μM) was added dropwise onto the film, and then let stand for 30 min. Finally, non-specific adsorption sites on the SPE surface were sealed with 10 μL of 6-mercapto-1-hexanol (MCH, 1 mM) [36]. After washing with PBS (0.1 M, pH 7.4), the disposable caspase-3 ECL biosensors were obtained. At the end of each step in the modification process, the SPE was rinsed with PBS (0.1 M, pH 7.4).

2.5. Cell apoptosis induction

MOLM-13 cells grown until the exponential phase were centrifuged at 1000 rpm for 10 min. The supernatant was discarded, and the cell pellets were dispersed in a fresh culture medium to a final concentration of 5.0×10^5 cells/mL determined using a cell counter. After that, 4 mL of the cell suspension was reacted with 2 μL of apoptosis-inducing reagent A (available in the apoptosis kit; was used as a positive control) to induce apoptosis for 0, 2, 4, 8, 12, 16 and 24 h. The cells were centrifuged to remove the culture medium and then washed once with PBS. After 100 μL of cell lysis buffer were added, and the cells were placed in an ice bath for 15 min. After the mixture was centrifuged at 13,000 rpm for 15 min at 4 °C, the supernatant was transferred to a new ice-cold centrifuge tube and then stored at −70 °C until subsequent use.

2.6. Determination of caspase-3 activity by ECL

After being added dropwise with caspase-3 at different concentrations or with cell lysate samples, the biosensors were placed in an incubator at 37 °C for 40 min. After washing with PBS (0.1 M, pH 7.4), the biosensors were immersed in PBS for ECL measurements. The continuous potential scanning of the biosensors was carried out from 0.2 to 1.3 V at a scanning rate of 0.1 V/s. The ECL signal was recorded by an MPI-A ECL analyzer, and the voltage of the photomultiplier tube (PMT)

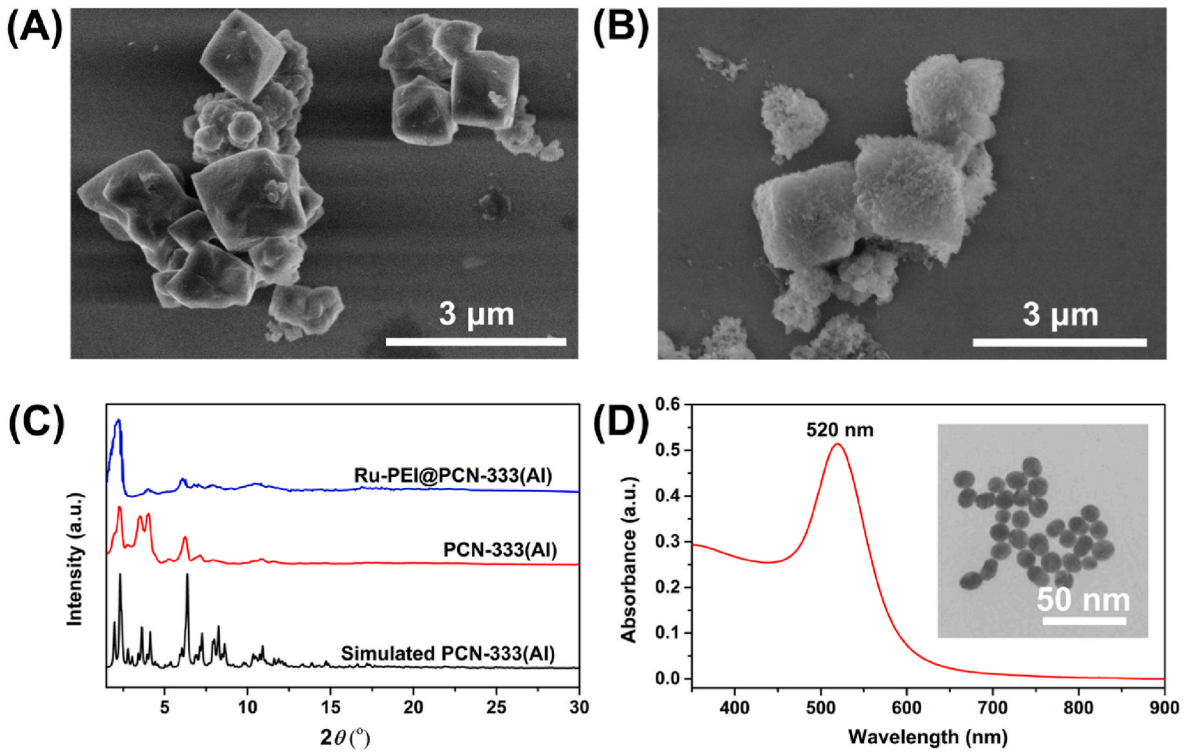

Fig. 1. (A–B) SEM images of PCN-333(Al) (A) and Ru-PEI@PCN-333(Al) (B). (C) Experimental XRD patterns of PCN-333(Al) and Ru-PEI@PCN-333(Al) and simulated XRD pattern of PCN-333(Al). (D) TEM image and UV–Vis spectrum of AuNPs.

was set at 800 V during the measurements.

3. Results and discussion

3.1. Characteristics of synthesized materials and SPEs

PCN-333(Al) has been demonstrated to be able to encapsulate a variety of enzymes including Cyt *c*, MP-11 and horseradish peroxidase, owing to its ultra-large cavity and ultra-high porosity [28,37,38]. In the present work, PCN-333(Al) was used as the scaffold to immobilize the Ru-PEI self-enhanced complex to construct the ternary Ru-PEI@PCN-333(Al) self-enhanced ECL system. In addition, PCN-333 (Al) was also used as an accelerator to enhance the ECL performance. Scanning electron microscopy (SEM) was employed to observe the morphology of PCN-333(Al) and Ru-PEI@PCN-333(Al), as shown in Fig. 1A and B. The prepared PCN-333(Al) had an octahedral shape. After the positively charged Ru-PEI was immobilized on its negatively charged surface via electrostatic adsorption, PCN-333(Al) became rough but its octahedral shape remained unchanged. The X-ray diffraction (XRD) patterns of PCN-333(Al) and Ru-PEI@PCN-333(Al) were almost completely overlapped with the simulated patterns generated using the single crystal diffraction simulation (Fig. 1C). These indicate the successful preparation of PCN-333(Al) and immobilization of Ru-PEI on the surface of PCN-333(Al). Transmission electron microscopy (TEM) and UV–Vis absorption spectroscopy were used to further characterize the prepared AuNPs. As depicted in Fig. 1D, the prepared AuNPs were uniformly distributed with a particle size of ~12 nm, and the characteristic absorption peak at 520 nm of AuNPs was observed.

SEM was used to characterize the surface of the working SPE. As shown in Figure S1, the bare working SPE was a carbon electrode comprising carbon particles evenly distributed on the surface. After being modified with AuNPs and Ru-PEI@PCN-333(Al) using CS as the binder, the surface of the electrode became concave and uneven. EDS mapping was employed to determine the distribution of the elements

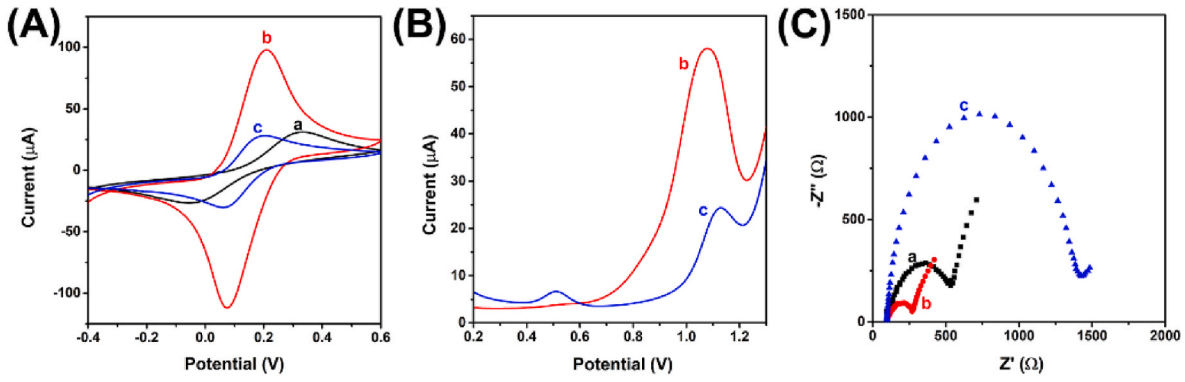

Fig. 2. (A) CV, (B) SWV, and (C) EIS of (a) bare SPE, (b) AuNPs/Ru-PEI@PCN-333(Al)/SPEs, and (c) Fc-peptide/AuNPs/Ru-PEI@PCN-333(Al)/SPEs. Cyclic voltammograms were measured in 5 mM $K_3[Fe(CN)_6]$ and 0.1 M KCl (pH 7.4). Square wave voltammograms were measured in 0.1 M PBS (pH 7.4). Electrochemical impedance spectra were measured in 1 mM $K_3[Fe(CN)_6]$, 1 mM $K_4[Fe(CN)_6]$ and 0.1 M KCl (pH 7.4).

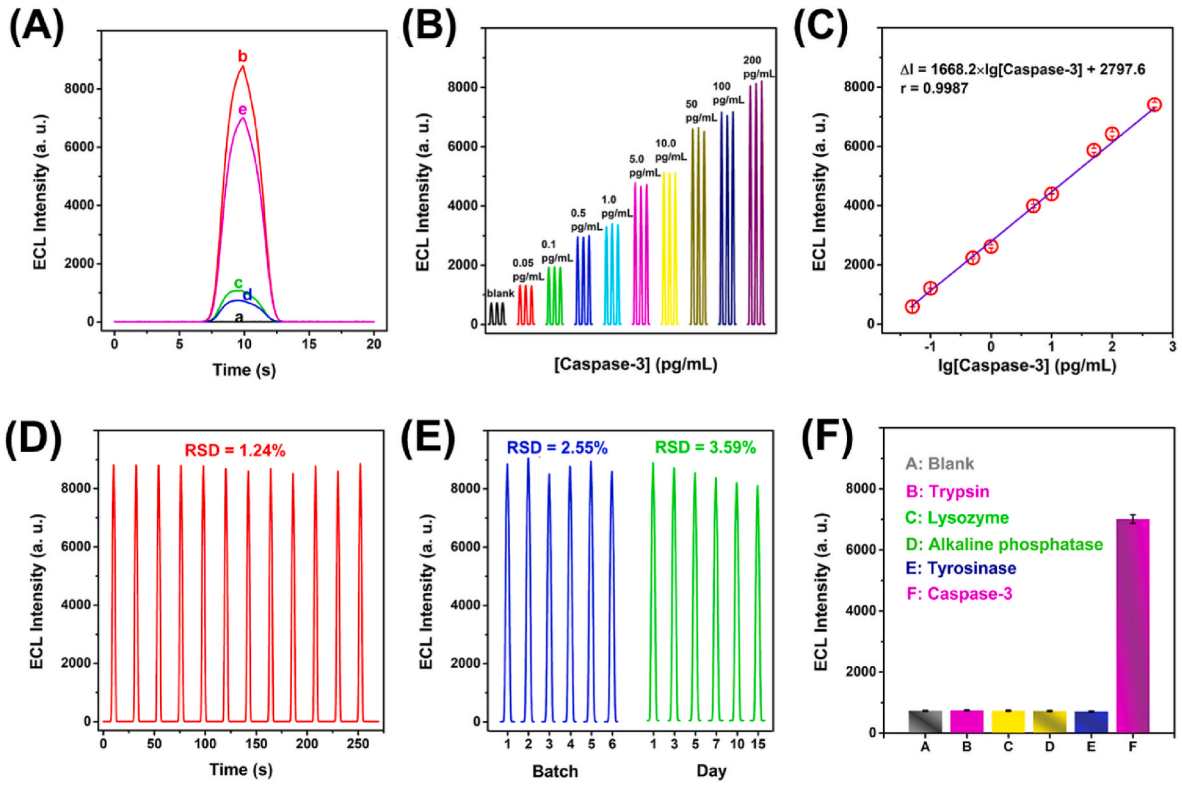

Fig. 3. (A) ECL signals of different modified electrodes: (a) bare SPE; (b) AuNPs/Ru-PEI@PCN-333(Al)/SPEs; (c) Fc-peptide/AuNPs/Ru-PEI@PCN-333(Al)/SPEs; (d) MCH/Fc-peptide/AuNPs/Ru-PEI@PCN-333(Al)/SPEs; and (e) MCH/Fc-peptide/AuNPs/Ru-PEI@PCN-333(Al)/SPEs in the presence of caspase-3 (100 pg/mL). (B) Response of ECL biosensor in the presence of caspase-3 at different concentrations. (C) Calibration curve of caspase-3 determination. (D–E) Stability of ECL signal of the prepared AuNPs/Ru-PEI@PCN-333(Al)/SPEs upon being subjected to continuous scanning for 12 cycles (D), and those from 6 batches or stored for 15 days (E). (F) Selectivity of ECL biosensor towards 100 pg/mL caspase-3 in the presence of 1000 pg/mL each of trypsin, lysozyme, alkaline phosphatase and tyrosinase (the incubation time of caspase-3 is 40 min).

including Al, Ru, and Au around the electrode. Using carbon as a reference, it can be seen that the three elements were evenly distributed on the working electrode, an indication that the electrode was uniformly modified by the three elements.

3.2. Electrochemical characteristics of the biosensor

The thiol group of terminal cysteine residue of the Fc-peptide can bind to AuNPs surface via Au–S bonds, allowing the Fc-peptide to be immobilized on AuNPs/Ru-PEI@PCN-333(Al)/SPEs. The AuNPs/Ru-PEI@PCN-333(Al) can enhance the efficiency of ECL by improving the charge transfer rate. The assembly process of the Fc-peptide/AuNPs/Ru-PEI@PCN-333(Al)/SPEs was characterized by cyclic voltammetry (CV), square wave voltammetry (SWV), and electrochemical impedance spectroscopy (EIS) (Fig. 2). Compared with that of the bare SPE, the CV peak current of the modified AuNPs/Ru-PEI@PCN-333(Al) was significantly higher, whereas the difference between its CV potential at the anode and the cathode was lower because of its excellent conductivity. This is consistent with the EIS results, in which the electron transfer resistance (Rct, reflected by the semicircle at higher frequencies) of the AuNPs/Ru-PEI@PCN-333(Al) composites was found to decrease after being modified. After being further immobilized with the Fc-peptide, the SWV showed that the current of Ru^{2+} at +1.1 V decreased and the characteristic oxidation peak of Fc at +0.5 V appeared. This indicates that the Fc-peptide was successfully immobilized on the AuNPs/Ru-PEI@PCN-333(Al)/SPEs, resulting in the inhibition of the electrochemical oxidation of Ru^{2+}, causing the quenching of ECL emission. Both the reduction of the CV peak current and the expansion of the EIS semicircle due to the inhibited electron transfer further indicate the successful immobilization of the Fc-peptide.

3.3. Performance of the ECL biosensor

The performance of the ECL-based biosensor was investigated (Fig. 3A). The ECL signal of bare SPEs in PBS was almost unobservable. But after the AuNPs/Ru-PEI@PCN-333(Al) was modified, it increased sharply. According to the literature [39,40], we speculate that the ECL emission mechanism of Ru-PEI@PCN-333(Al) may be as follows:

$$[Ru^{2+}\text{-PEI@PCN-333(Al)}] - e^- \rightarrow [Ru^{3+}\text{-PEI@PCN-333(Al)}]$$

$$PEI - e^- \rightarrow PEI^{+\cdot}$$

$$PEI^{+\cdot} \rightarrow PEI\cdot + H^+$$

$$[Ru^{3+}\text{-PEI@PCN-333(Al)}] + PEI\cdot \rightarrow [Ru^{2+}\text{-PEI@PCN-333(Al)}]^* + PEI$$

$$[Ru^{2+}\text{-PEI@PCN-333(Al)}]^* \rightarrow [Ru^{2+}\text{-PEI@PCN-333(Al)}] + h\nu$$

After the immobilization with the Fc-peptide, the ECL signal of the modified SPEs decreased significantly, suggesting that the ECL emission of Ru^{2+} can be quenched by Fc-peptide. After MCH was dropped onto SPEs to block the remaining active sites, the ECL signal further decreased. After the biosensor was incubated with 100 pg/mL caspase-3, which was added dropwise, the ECL signal significantly increased. This suggests that the Fc-peptide containing the caspase-3 recognition site (Asp-Glu-Val-Asp) was successfully cleaved by caspase-3 and then diffused away from the electrode surface; as a result, the ECL signal was recovered. These results indicate that the ECL-based caspase-3 biosensor was successfully fabricated.

Table 1
Comparison of different methods used for the detection of caspase-3 activity.

Method	System	LOD (pg/mL)	References
Colorimetry	Unlabeled peptide substrate and unmodified AuNPs	1×10^4	[41]
Surface enhanced Raman spectroscopy	AuNP-peptide probe	1.5×10^3	[42]
Chemiluminescent	N-(4-aminobutyl)-N-ethylisoluminol-labeled peptide forming the magnetic beads	300	[43]
Fluorescence	$NaErF_4$:Tm^{3+}@$NaYbF_4$@$NaYF_4$:Nd^{3+} UCNPs@ polydopamine@Cy3-peptide	65	[44]
Fluorescence	Ac-Tat-DEVD-cresyl violet	5.3	[45]
Electrochemistry	Peptide-Cu(II)/GO	0.2	[46]
ECL	MCH/biotin-DEVD-peptide/AuNPs/PDDA/CNTs/GCE	0.07	[47]
ECL	MCH/Fc-peptide/AuNPs/Ru-PEI@PCN-333(Al)/SPEs	0.017	This work

3.4. Optimal experimental conditions

After being immobilized with the Fc-peptide, the AuNPs/Ru-PEI@PCN-333(Al)-modified SPEs were employed to detect caspase-3 in cell lysates. Caspase-3 can act as a switch to turn on the ECL emission of the biosensor after it selectively cleaves the N-terminus of the Fc-peptide. Incubation times during the immobilization of Fc-peptide and during its cleavage by caspase-3 were optimized. As shown in Figure S2, for the immobilization of Fc-peptide, the ECL signal gradually decreased and finally began to level off after 30 min; thus, 30 min was selected as the optimal incubation time for the immobilization of Fc-peptide. For the cleavage of Fc-peptide by caspase-3, the ECL signal increased and became stable after 40 min. Therefore, 40 min was chosen as the appropriate incubation time for the cleavage of Fc-peptide by caspase-3.

3.5. Performance in caspase-3 activity determination of the biosensor

To ensure that it can be used to quantitatively determine caspase-3 activity, the fabricated ECL biosensor was employed to detect caspase-3 at different concentrations, as shown in Fig. 3B. The relationship between the change in the ECL intensity (ΔI) and the logarithmic value of caspase-3 concentration was linear with an equation: $\Delta I = 1668.2 \lg$ [caspase-3] + 2797.6 (r = 0.9987) (Fig. 3C). The LOD of our sensor was determined to be 0.017 pg/mL (3σ), which is, to the best of our knowledge, the lowest LOD ever reported, and its sensitivity was also higher than that of other methods reported in the literature (Table 1). The stability, reproducibility and selectivity of the biosensor were also investigated (Fig. 3D–F). After 12 consecutive potential scanning cycles, the ECL signal of AuNPs/Ru-PEI@PCN-333(Al)/SPEs was not significantly changed (the relative standard deviation (RSD) was less than 2%). The ECL signals of six AuNPs/Ru-PEI@PCN-333(Al)-modified SPEs from six different batches and one AuNPs/Ru-PEI@PCN-333(Al)-modified SPE from six-time nodes during 15-day storage in a desiccator under darkness were also not significantly changed with RSDs of less than 3.5% and 5%, respectively. These data prove that the fabricated biosensor has good stability and reproducibility. To evaluate the selectivity of the biosensor, the interference by proteins including trypsin, lysozyme, alkaline phosphatase and tyrosinase were examined. The ECL results showed that these proteins almost had no interfering effects, indicating that the biosensor has high selectivity.

3.6. Performance of ECL biosensor in determining caspase-3 activity in MOLM-13 cells by apoptosis inducer

The expression of caspase-3 in MOLM-13 cells (model cells) was induced by an apoptosis inducer. The changes of time-dependent ECL intensity caused by caspase-3 in MOLM-13 cell lysates were recorded for 24 h, as shown in Fig. 4A. With increasing apoptosis induction time, the ECL signal increased and became stable after 12 h, which is in accordance with the results from colorimetric experiment. This indicates that the proposed ECL biosensor can be used to monitor caspase-3 activity during apoptosis. To further assess the specificity of the ECL biosensor, a caspase-3 inhibitor Ac-DEVD-CHO was used to inhibit the activity of caspase-3. As shown in Fig. 4B, with increasing inhibitor concentration, the ECL signal gradually decreased. The results further confirm that the change of ECL intensity is due to caspase-3 activity and that the ECL biosensor can reliably be used to monitor caspase-3 activity during the cell apoptosis.

3.7. Performance of ECL biosensor in determining caspase-3 activity in acute myeloid leukemia cells induced by anticancer drugs

The ability of the ECL biosensor to determine caspase-3 activity in acute myeloid leukemia cells, of which the apoptosis was induced using two anticancer drugs, daunorubicin and adriamycin, was evaluated. The cells were pretreated with the two drugs to induce the apoptosis for 12 h, and their ECL intensities were then measured. As illustrated in Fig. 4C, the increase of drug concentration caused the ECL signal of the biosensor to gradually increase, an indication that the apoptosis of acute myeloid leukemia cells was induced by the anticancer drugs, and the amount of caspase-3 increased as the induction time increased. After 12 h, the cells have completely apoptotic and couldn't release more caspase-3, so the

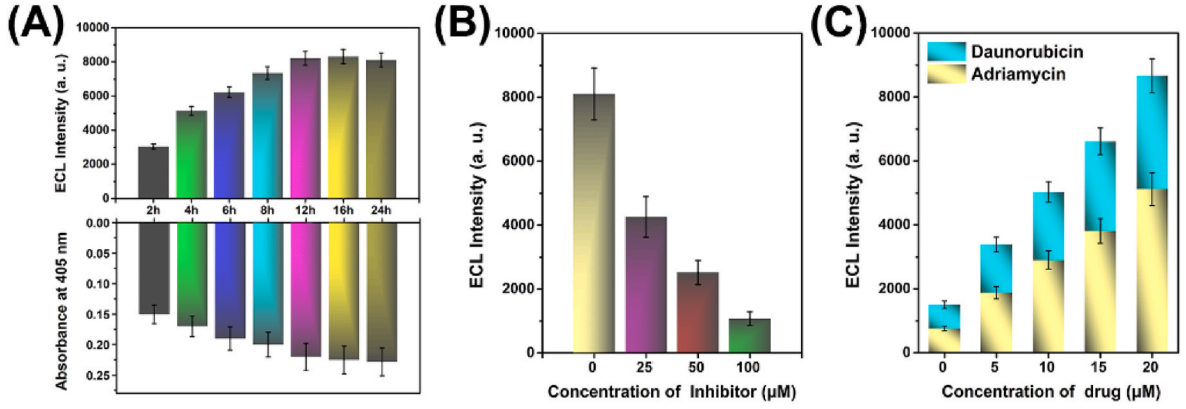

Fig. 4. (A) ECL measurements (top) and colorimetric assay (bottom) of caspase-3 activity in MOLM-13 cells incubated with an apoptosis inducer for different times: 0, 2, 4, 6, 8, 12, 16, and 24 h. (B) ECL measurements of caspase-3 activity in the presence of Ac-DEVD-CHO inhibitor at different concentrations. (C) Concentration-dependent caspase-3 activity induced by anticancer drugs, daunorubicin and adriamycin.

ECL intensity reaches the plateau area. Additionally, daunorubicin at a lower concentration was required to achieve the same degree of apoptosis as that of adriamycin. These results indicate that the proposed biosensor can effectively and sensitively monitor caspase-3 activity induced by anticancer drugs in acute myeloid leukemia cells.

4. Conclusions

In summary, a disposable biosensor based on a novel ternary Ru-PEI@PCN-333(Al) self-enhanced ECL system for on-site caspase-3 activity determination was developed for the first time. The ECL biosensor could successfully monitor caspase-3 activity during cell apoptosis and had excellent performance. With the use of solid-state ECL strategy and due to the quenching effect of Fc-peptide on the ECL emission of Ru^{2+}, the biosensor had high sensitivity with an LOD of 0.017 pg/mL, as well as outstanding stability, reproducibility and selectivity. The ECL biosensor was successfully employed to detect apoptosis of acute myeloid leukemia cells induced by two anticancer drugs, daunorubicin and adriamycin. The introduction of disposable screen-printed electrodes (SPEs) provided the biosensor with on-site, rapid caspase-3 activity determination capability. This work lays a foundation for the development of more advanced portable ECL biosensing devices that can reliably detect not only caspase-3, but also other bioanalytes.

Credit author statement

Weiwei Luo: Conceptualization, Data curation, Formal analysis, Investigation, Writing-original draft. Hongyu Chu: Data curation, Investigation. Xinzhao Wu: Writing-review & editing, Formal analysis. Pinyi Ma: Conceptualization, Project administration, Data curation, Writing-review & editing. Qiong Wu: Investigation, Resources, Writing-review. Daqian Song: Project administration, Funding acquisition, Resources, Supervision.

Declaration of competing interest

The authors declare that they have no known competing financial interests or personal relationships that could have appeared to influence the work reported in this paper.

Acknowledgments

This work was supported by the National Natural Science Foundation of China (Grant Nos. 22074052 and 22004046).

Appendix A. Supplementary data

Supplementary data to this article can be found online at https://doi.org/10.1016/j.talanta.2021.123083.

References

[1] L. Wu, X. Qu, Cancer biomarker detection: recent achievements and challenges, Chem. Soc. Rev. 44 (2015) 2963–2997.
[2] I.M. Ghobrial, T.E. Witzig, A.A. Adjei, Targeting apoptosis pathways in cancer therapy, CA, Can. J. Clinic. 55 (2005) 178–194.
[3] S. Fulda, Molecular pathways: targeting inhibitor of apoptosis proteins in cancer—from molecular mechanism to therapeutic application, Clin. Cancer Res. 20 (2014) 289–295.
[4] B.A. Carneiro, W.S. El-Deiry, Targeting apoptosis in cancer therapy, Nat. Rev. Clin. Oncol. 17 (2020) 395–417.
[5] S. Takano, S. Shiomoto, K.Y. Inoue, K. Ino, H. Shiku, T. Matsue, Electrochemical approach for the development of a simple method for detecting cell apoptosis based on caspase-3 activity, Anal. Chem. 86 (2014) 4723–4728.
[6] Y.-P. Dong, G. Chen, Y. Zhou, J.-J. Zhu, Electrochemiluminescent sensing for caspase-3 activity based on Ru(bpy)32+-Doped silica nanoprobe, Anal. Chem. 88 (2016) 1922–1929.
[7] D. Su, X. Hu, C. Dong, J. Ren, Determination of caspase-3 activity and its inhibition constant by combination of fluorescence correlation spectroscopy with a microwell chip, Anal. Chem. 89 (2017) 9788–9796.
[8] B. Khalilzadeh, N. Shadjou, H.N. Charoudeh, M.-R. Rashidi, Recent advances in electrochemical and electrochemiluminescence based determination of the activity of caspase-3, Microchimica Acta 184 (2017) 3651–3662.
[9] T.-I. Kim, H. Jin, J. Bae, Y. Kim, Excimer emission-based fluorescent probe targeting caspase-3, Anal. Chem. 89 (2017) 10565–10569.
[10] R. Yang, Y. Li, K. Zou, L. Meng, X. Zhang, J. Chen, A label-free and blocker-free photoelectrochemical strategy for highly sensitive caspase-3 assay, Chem. Commun. 54 (2018) 4830–4833.
[11] Z. Zhou, L. Peng, X. Wang, Y. Xiang, A. Tong, A new colorimetric strategy for monitoring caspase 3 activity by HRP-mimicking DNAzyme–peptide conjugates, Analyst 139 (2014) 1178–1183.
[12] J. Li, X. Li, X. Shi, X. He, W. Wei, N. Ma, et al., Highly sensitive detection of caspase-3 activities via a nonconjugated gold nanoparticle–quantum dot pair mediated by an inner-filter effect, ACS Appl. Mater. Interfaces 5 (2013) 9798–9802.
[13] Y. Li, Chemiluminescent determination of the activity of caspase-3 using a specific peptide substrate and magnetic beads, Microchimica Acta 177 (2012) 443–447.
[14] D. Deng, Y. Hao, S. Yang, Q. Han, L. Liu, Y. Xiang, et al., A signal-on electrochemical biosensor for evaluation of caspase-3 activity and cell apoptosis by the generation of molecular electrocatalysts on graphene electrode surface for water oxidation, Sensor. Actuator. B Chem. 286 (2019) 415–420.
[15] W. Miao, Electrogenerated chemiluminescence and its biorelated applications, Chem. Rev. 108 (2008) 2506–2553.
[16] L. Hu, G. Xu, Applications and trends in electrochemiluminescence, Chem. Soc. Rev. 39 (2010) 3275–3304.
[17] Z. Liu, W. Qi, G. Xu, Recent advances in electrochemiluminescence, Chem. Soc. Rev. 44 (2015) 3117–3142.
[18] B. Khalilzadeh, N. Shadjou, H. Afsharan, M. Eskandani, H. Nozad Charoudeh, M.-R. Rashidi, Reduced graphene oxide decorated with gold nanoparticle as signal amplification element on ultra-sensitive electrochemiluminescence determination of caspase-3 activity and apoptosis using peptide based biosensor, Bioimpacts 6 135-147.
[19] H. Wang, Y. He, Y. Chai, R. Yuan, A super intramolecular self-enhanced electrochemiluminescence immunosensor based on polymer chains grafted on palladium nanocages, Nanoscale 6 (2014) 10316–10322.
[20] Y. Zhuo, N. Liao, Y.-Q. Chai, G.-F. Gui, M. Zhao, J. Han, et al., Ultrasensitive apurinic/apyrimidinic endonuclease 1 immunosensing based on self-enhanced electrochemiluminescence of a Ru(II) complex, Anal. Chem. 86 (2014) 1053–1060.
[21] X. Jiang, H. Wang, H. Wang, Y. Zhuo, R. Yuan, Y. Chai, Self-enhanced N-(aminobutyl)-N-(ethylisoluminol) derivative-based electrochemiluminescence immunosensor for sensitive laminin detection using PdIr cubes as a mimic peroxidase, Nanoscale 8 (2016) 8017–8023.
[22] F. Yang, X. Zhong, X. Jiang, Y. Zhuo, R. Yuan, S. Wei, An ultrasensitive aptasensor based on self-enhanced Au nanoclusters as highly efficient electrochemiluminescence indicator and multi-site landing DNA walker as signal amplification, Biosens. Bioelectron. 130 (2019) 262–268.
[23] N. Cao, F. Zhao, B. Zeng, A novel self-enhanced electrochemiluminescence sensor based on PEI-CdS/Au@SiO2@RuDS and molecularly imprinted polymer for the highly sensitive detection of creatinine, Sensor. Actuator. B Chem. 306 (2020) 127591.
[24] J. Ye, G. Liu, M. Yan, Q. Zhu, L. Zhu, J. Huang, et al., Highly luminescent and self-enhanced electrochemiluminescence of tris(bipyridine) ruthenium(II) nanohybrid and its sensing application for label-free detection of MicroRNA, Anal. Chem. 91 (2019) 13237–13243.
[25] X. Liao, H. Fu, T. Yan, J. Lei, Electroactive metal–organic framework composites: design and biosensing application, Biosens. Bioelectron. 146 (2019) 111743.
[26] J. Zhou, Y. Li, W. Wang, X. Tan, Z. Lu, H. Han, Metal-organic frameworks-based sensitive electrochemiluminescence biosensing, Biosens. Bioelectron. 164 (2020) 112332.
[27] S. Zhang, F. Rong, C. Guo, F. Duan, L. He, M. Wang, et al., Metal–organic frameworks (MOFs) based electrochemical biosensors for early cancer diagnosis in vitro, Coord. Chem. Rev. 439 (2021) 213948.
[28] D. Feng, T.-F. Liu, J. Su, M. Bosch, Z. Wei, W. Wan, et al., Stable metal-organic frameworks containing single-molecule traps for enzyme encapsulation, Nat. Commun. 6 (2015) 5979.
[29] V. Gubala, L.F. Harris, A.J. Ricco, M.X. Tan, D.E. Williams, Point of care diagnostics: status and future, Anal. Chem. 84 (2012) 487–515.
[30] W. Gao, M. Saqib, L. Qi, W. Zhang, G. Xu, Recent advances in electrochemiluminescence devices for point-of-care testing, Curr. Opin. Electrochem. 3 (2017) 4–10.
[31] E. Martínez-Periñán, C. Gutiérrez-Sánchez, T. García-Mendiola, E. Lorenzo, Electrochemiluminescence biosensors using screen-printed electrodes, Biosensors 10 (2020) 118.
[32] S.K. Vashist, P.B. Luppa, L.Y. Yeo, A. Ozcan, J.H.T. Luong, Emerging technologies for next-generation point-of-care testing, Trends Biotechnol. 33 (2015) 692–705.
[33] W. Cao, J.P. Ferrance, J. Demas, J.P. Landers, Quenching of the electrochemiluminescence of tris(2,2′-bipyridine)ruthenium(II) by ferrocene and its potential application to quantitative DNA detection, J. Am. Chem. Soc. 128 (2006) 7572–7578.
[34] Y. Shi, C. Yi, Z. Zhang, H. Zhang, M. Li, M. Yang, et al., Peptide-bridged assembly of hybrid nanomaterial and its application for caspase-3 detection, ACS Appl. Mater. Interfaces 5 (2013) 6494–6501.
[35] K. Fu, R. Zhang, J. He, H. Bai, G. Zhang, Sensitive detection of ketamine with an electrochemical sensor based on UV-induced polymerized molecularly imprinted membranes at graphene and MOFs modified electrode, Biosens. Bioelectron. 143 (2019) 111636.

[36] H. Xiao, L. Liu, F. Meng, J. Huang, G. Li, Electrochemical approach to detect apoptosis, Anal. Chem. 80 (2008) 5272–5275.
[37] V. Lykourinou, Y. Chen, X.-S. Wang, L. Meng, T. Hoang, L.-J. Ming, et al., Immobilization of MP-11 into a mesoporous metal–organic framework, MP-11@mesoMOF: a new platform for enzymatic catalysis, J. Am. Chem. Soc. 133 (2011) 10382–10385.
[38] D.S. Raja, W.-L. Liu, H.-Y. Huang, C.-H. Lin, Immobilization of protein on nanoporous metal-organic framework materials, Comments Mod. Chem. 35 (2015) 331–349.
[39] Y. Yang, G.-B. Hu, W.-B. Liang, L.-Y. Yao, W. Huang, R. Yuan, et al., A highly sensitive self-enhanced aptasensor based on a stable ultrathin 2D metal-organic layer with outstanding electrochemiluminescence property, Nanoscale 11 (2019) 10056–10063.
[40] G.-B. Hu, C.-Y. Xiong, W.-B. Liang, X.-S. Zeng, H.-L. Xu, Y. Yang, et al., Highly stable mesoporous luminescence-functionalized MOF with excellent electrochemiluminescence property for ultrasensitive immunosensor construction, ACS Appl. Mater. Interfaces 10 (2018) 15913–15919.
[41] Y. Pan, M. Guo, Z. Nie, Y. Huang, Y. Peng, A. Liu, et al., Colorimetric detection of apoptosis based on caspase-3 activity assay using unmodified gold nanoparticles, Chem. Commun. 48 (2012) 997–999.
[42] C. Zhao, L. Qiu, P. Lv, A. Han, G. Fang, J. Liu, et al., AuNP-peptide probe for caspase-3 detection in living cells by SERS, Analyst 144 (2019) 1275–1281.
[43] Y. Li, Chemiluminescent determination of the activity of caspase-3 using a specific peptide substrate and magnetic beads, Microchimica Acta 177 (2012) 443–447.
[44] L. Liu, X. Li, H. Zhang, H. Chen, M.M.A. Abualrejal, D. Song, et al., Six-in-One peptide functionalized Upconversion@Polydopamine nanoparticle-based ratiometric fluorescence sensing platform for real-time evaluating anticancer efficacy through monitoring caspase-3 activity, Sensor. Actuator. B Chem. 333 (2021) 129554.
[45] Y. Jin, K. Xu, Y. Huang, H. Zhong, R. Zhao, Activity-based probe for ratiometric fluorescence imaging of caspase-3 in living cells, Anal. Chem. 93 (2020) 2045–2052.
[46] D. Deng, Y. Hao, S. Yang, Q. Han, L. Liu, Y. Xiang, et al., A signal-on electrochemical biosensor for evaluation of caspase-3 activity and cell apoptosis by the generation of molecular electrocatalysts on graphene electrode surface for water oxidation, Sens. Actuat. B Chem. 286 (2019) 415–420.
[47] Y.-P. Dong, G. Chen, Y. Zhou, J.-J. Zhu, Electrochemiluminescent sensing for caspase-3 activity based on Ru(bpy)32+-Doped silica nanoprobe, Anal. Chem. 88 (2016) 1922–1929.